STEM CELLS AND DEVELOPMENT
Volume 21, Number 9, 2012

DOI: 10.1089/scd.2011.0244

Adipose Tissue-Derived Stem Cells Ameliorate Diabetic Bladder Dysfunction in a Type II Diabetic Rat Model

Haiyang Zhang,[1,2] Xuefeng Qiu,[2] Alan W. Shindel,[3] Hongxiu Ning,[2] Ludovic Ferretti,[2] Xunbo Jin,[1] Guiting Lin,[2] Ching-Shwun Lin,[2] and Tom F. Lue[2]

Diabetes mellitus is associated with a broad constellation of voiding complaints that are often multifactorial and resistant to currently available therapies. The leading causes of diabetic bladder dysfunction (DBD) include alterations in the bladder smooth muscle, neuronal degeneration, and urothelial dysfunction. Adipose tissue-derived stem cells (ADSCs), a type of mesenchymal stromal cells, have shown promise as a novel tissue regenerative technique that may have utility in DBD. The aim of this study is to determine the efficacy and mechanism by which ADSCs may ameliorate DBD in rats fed a high-fat diet and treated with low-dose streptozotocin to induce type II diabetes. Improved voiding function was noted in ADSCs-treated rats as compared with phosphate-buffered saline-treated rats. Though some ADSCs differentiated into smooth muscle cells, paracrine pathway seems to play a main role in this process, thus resulting in reduction of apoptosis and preservation of "suburothelial capillaries network."

Introduction

Diabetic bladder dysfunction (DBD) refers to a range of voiding complaints that are prevalent in men and women with diabetes mellitus (DM) [1]. Based on both animal studies and human findings, Daneshgari et al. [1] proposed that DBD typically evolves in a time-dependent progression of both storage and voiding problems. The early phase of DBD manifests as detrusor overactivity, thus leading to urinary frequency and urgency. Over time, progressive oxidative stress and neuropathy lead to decompensation of the detrusor musculature, thereby leading to the hypocontractile or atonic bladder. The protean nature of DBD is due in large part to the numerous physiological insults that may occur in the diabetic state, including alteration in smooth muscle cells (SMCs) activity, neuropathy, and urothelial dysfunction [2].

There are many treatment options for voiding symptoms that may be applied to patients with DBD; however, patients with diabetes are often refractory to management due to low response to therapy or high recurrence rates. Existing treatments are also limited in that they are designed to mitigate symptoms rather than treat the underlying disorder. Novel paradigms for treating the underlying the disease processes of DBD have been explored in recent investigations, including supplementation of nerve growth factor therapy [3,4], and N-hexacosanol therapy [5].

Adipose tissue-derived stem cells (ADSCs) are mesenchymal stromal cells (MSCs) found in the perivascular space of adipose tissue. These cells have the advantage of abundance and easy access when compared with other stem cell types [6]. ADSCs express common stem cell surface markers, genes, and differentiation potentials as mesenchymal stem cells [7]. ADSCs have demonstrated efficacy in preclinical studies of a range of urologic conditions [8–11]. Although efficacy in these animal models has been demonstrated, many questions remain. Of particular importance is the mechanisms by which these cells exert their effect; there is evidence that paracrine pathways may be more important than direct cellular differentiation [8].

In the current study, we first investigated the utility of ADSCs therapy for DBD in a type II DM rat model induced by a high-fat diet (HFD) and low-dose streptozotocin (STZ). Our goals were (1) to study DBD in a rat model of type II diabetes; (2) to examine the effects of ADSC on DBD; and (3) to assess both cellular differentiation and paracrine effect of ADSCs after implantation.

Our hypothesis was that ADSCs would ameliorate voiding dysfunction in this rat model system of diabetes; we further hypothesized that better voiding function would be associated with paracrine pathways of ADSCs.

Materials and Methods

Experimental design

Thirty-nine female Sprague-Dawley rats (8 weeks old) were obtained from Charles River Laboratories. All animal

[1]Minimally Invasive Urology Center, Provincial Hospital Affiliated to Shandong University, Jinan, China.
[2]Knuppe Molecular Urology Laboratory, Department of Urology, School of Medicine, University of California, San Francisco, San Francisco, California.
[3]Department of Urology, University of California, Davis, California.

care, treatments, and procedures were approved by our Institutional Animal Care and Use Committee.

All rats were given tap water *ad libitum* and maintained in a temperature- and humidity-controlled room on 12-h light/dark cycles. Ten rats fed with standard rat chow served as the control group. The remaining 29 rats (Diabetic group) were given a HFD (Zeigler Brothers) for 1 month, followed by 2 intraperitoneal injections of STZ (Sigma-Aldrich) at 30 mg/kg separated by 1 week [12]. The rats were allowed to continue to feed on their respective diets until the end of the study. Body weight and fasting blood glucose (rats were fasted for 12 h before measurement) were monitored every week. Only rats with fasting blood glucose ≥ 140 mg/dL were considered diabetic and used in subsequent portions of the study.

Three months after STZ treatment, an insulin tolerance test was performed as detailed next to assess the insulin sensitivity of each group. All animals in each group then underwent harvest of paragonadal fat via laparotomy for procurement ADSCs as previously described [7]. ADSCs were processed and labeled with 10 μM 5-ethynyl-2-deoxyuridine (EdU; Invitrogen). The 29 diabetic rats in the diabetic group were randomly divided into 3 groups; group 1 received an injection of phosphate-buffered saline (PBS) 1 mL into the detrusor via repeat laparotomy (DM + PBS group, $n = 9$); group 2 received 3×10^6 autologous ADSCs in 0.5 mL PBS via tail vein injection (DM + T group, $n = 10$); and group 3 received 3×10^6 autologous ADSCs in 1 mL PBS by an injection into the detrusor at the time of repeat laparotomy (DM + B group, $n = 10$). Rats in the control group received 1 mL PBS in the detrusor via laparotomy (N + PBS group, $n = 10$).

One month after treatment, all rats underwent conscious cystometry and were sacrificed for histology analysis.

ADSCs harvest and processing, EdU labeling, and then injection

ADSCs were harvested and cultured according to a standardized protocol [13,14]. The ADSCs cultured with this technique were extensively characterized in previous studies [7]. For tracking, ADSCs were treated with 10 μM EdU overnight before the injection. A total of 3×10^6 EdU labeled ADSCs were collected into a 2 mL conical tube containing 1 mL or 0.5 mL PBS and used for an injection.

ADSCs injection was performed according to previous protocol [10]. All rats were anesthetized with isoflurane and underwent midline laparotomy to expose the bladder. Rats underwent an injection of 1 mL PBS (N + PBS and DM + PBS groups) or 3 million autologous ADSCs in 1 mL PBS (DM + B group) in the bladder. After treatment, the incision was closed in 2 layers. DM + T rats received 3 million autologous ADSCs transplanted via the tail vein.

Plasma insulin tolerance test

Three months after STZ injection, all rats underwent plasma insulin tolerance test as previously described [12]. Insulin (1 IU/kg; Sigma-Aldrich) was administered by intraperitoneal injection, and blood samples from the tail vein were collected at 0, 15, 30, 60, 90, and 120 min for the measurement of plasma glucose. The value is presented as a percentage of initial plasma glucose level.

Conscious cystometry

Awake cystometry was performed as previously described [10,15]. Under isoflurane anesthesia, a polyethylene-90 catheter was implanted into the bladder 24 h before conscious cystometry. A second polyethylene-90 tube attached to a latex balloon was placed in the intra-abdominal space to measure abdominal pressure. At the time of cystometry, the bladder was filled via the bladder catheter with room-temperature PBS at 0.1 mL/min while recording simultaneous pressure in the bladder and abdomen with Laboratory View 6.0 software. Rats were allowed about 20 min for the voiding pattern to stabilize. Thereafter, micturition was recorded for 1 h.

Measurement of plasma biochemistry

After euthanasia, 1 mL blood was collected into a tube containing heparin (20 μL, 200 IU/mL; Celsus) by puncture of the inferior vena cava. Plasma was separated by centrifugation at 3,500 g for 10 min. Plasma insulin, triglyceride (TG), high density lipoprotein (HDL), and low/very low density lipoprotein (LDL/VLDL) were measured by commercial insulin enzyme-linked immunosorbent assay (ELISA) kit (Millipore) and TG, HDL, LDL/VLDL quantification kit (BioVision) according to the instructions, respectively.

Immunofluorescence and Immunohistochemical staining

Bladder tissue preparation, immunofluorescence, and immunohistochemical staining were performed according to our previous protocols [16]. Five rats were randomly chosen from each group for histological studies. Primary antibodies included mouse anti-smooth muscle actin (SMA; Abcam), rabbit anti-collagen IV (Col IV; Abcam), goat anti-uroplakin II (UP II; Santa Cruz Biotechnology), mouse anti-rat endothelial cell antigen-1 (RECA-1; AbD Serotec), and mouse anti-stromal cell-derived factor-1 (SDF-1; Santa Cruz Biotechnology). RECA-1 staining was performed with the avidin-biotin-peroxidase method by using the Vectastain Elite ABC (Vector Laboratories, Inc.) with 3,3-diaminobenzidine as the chromagen. All other antibody staining used secondary antibody conjugated with Alexa-488 fluor or Texas Red. Actin was also stained by incubation over 20 min with phalloidin (Invitrogen) in 4% paraformaldehyde.

For tracking ADSCs, tissue sections were incubated with Click-IT reaction cocktail (Invitrogen) for 30 min at room temperature.

Quantification of apoptotic cells and EdU-retaining cells in bladder tissue

Quantification of apoptotic cells in bladder tissue was performed by detecting DNA damage *in-situ* using TUNEL kit (BD Pharmingen) staining according to the instruction and counterstaining by 4′,6-diamidino-2-phenylindole (DAPI; Sigma-Aldrich). After TUNEL staining, the slides were evaluated by using fluorescence microscopy, and the number of apoptotic nuclei (in mucosal layer and in muscular layer, respectively) was counted by Image Pro Plus software (Media Cybernetics). To generate statistically relevant data, 3 high-power microscopic fields were counted in each sample of 5 rats in respective groups.

The approximate number of EdU-retaining ADSCs in each bladder (in submucosal layer and in muscular layer, respectively) was calculated by multiplying the number of EdU-expressing ADSCs in one section, and the number of sections in one bladder could be cut. The number of EdU-expressing ADSCs in one section was counted by Image Pro Plus software. The number of sections in one bladder that could be cut was calculated by dividing the thickness of the whole bladder (after fixation in 2% formaldehyde) with the thickness of one section (5 μm). To generate statistically relevant data, EdU-retaining ADSCs were counted and calculated in 5 samples from DM + T and DM + B group.

Quantification of vascular endothelial growth factor secretion

For quantification of secreted vascular endothelial growth factor (VEGF), rat ADSCs and penile smooth muscle cells (PSMCs) were treated as previously described [17]. To ensure unbiased assessment, all the processed culture media were simultaneously subjected to ELISA for VEGF with a commercial kit (R&D Systems). To generate statistically relevant data, each cell medium was subjected to 3 independent ELISA experiments, and each ELISA experiment included triplicates of each cell medium.

Determination of apoptosis of cells in vitro, and matrigel-based capillary-like tube formation assay

Please see in Supplementary Materials and Methods file; Supplementary Data are available online at www.liebertonline.com/scd.

Statistical analysis

Data were analyzed with Prism 5 (GraphPad Software, Inc.) and expressed as mean ± standard error of the mean for continuous variables. Continuous data were compared among the groups by using one-way analysis of variance. The Tukey–Kramer test was used for *post-hoc* comparisons. To evaluate the effect of ADSCs among the groups, Chi-Square test was performed with Fisher's Exact Test. Statistical significance was set at $P < 0.05$.

Results

Animals in the diabetic group had higher mean body weight (Fig. 1A), lower insulin sensitivity (Fig. 1B), modest reduction of plasma insulin, significantly higher plasma glucose level, and more dyslipidemia (Table 1) relative to the control group. We posit that these animals closely resemble

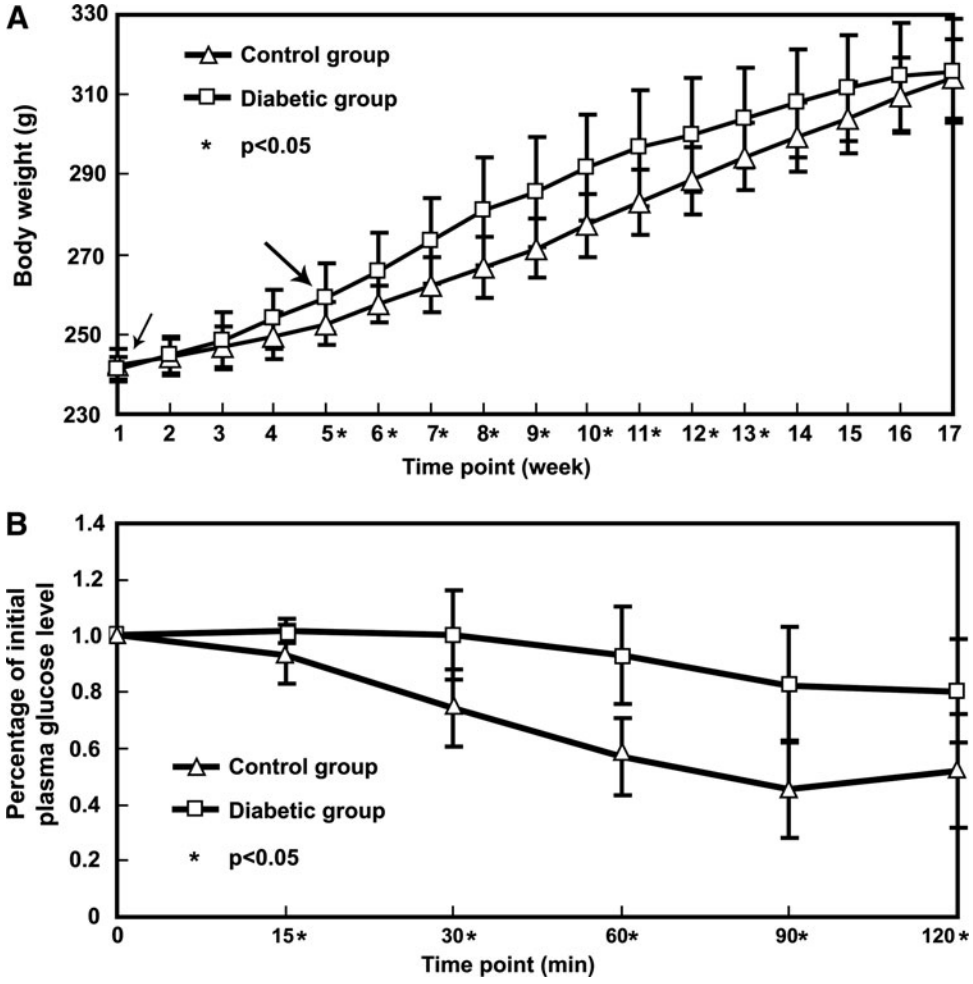

FIG. 1. **(A)** Body weights in 2 groups were monitored every week. The rats in diabetic groups were fed high-fat food from the beginning of the study (*small arrowhead*). One month later, all rats in the diabetic groups received streptozotocin injections (*large arrowhead*). **(B)** Insulin tolerance test. Insulin sensitivity was assessed by the percentage of initial plasma glucose level at different time points after an insulin injection. Insulin resistance was noted in the diabetic group.

Table 1. Plasma Biochemistry

Groups	*N+PBS (n=10)*	*DM+PBS (n=9)*	*DM+T (n=10)*	*DM+B (n=10)*	P *value*
Plasma glucose (mg/dL)	103.7±10.4[a]	376.8±125.7	370±132.7	389.1±87.9	<0.001
Insulin (pM)	198.6±38.1	172.2±47.5	177.2±29.7	193.5±49.8	=0.653
Triglyceride (mM)	1.13±0.46[a]	7.17±2.59	6.29±2.74	6.48±3.39	<0.001
LDL/VLDL (μg/μL)	0.15±0.06[a]	0.76±0.24	0.79±0.27	0.83±0.32	<0.001
HDL (μg/μL)	0.51±0.09	0.47±0.13	0.40±0.11	0.45±0.24	=0.481

[a]$P<0.001$ versus other groups.
LDL/VLDL, low/very low density lipoprotein; HDL, high density lipoprotein; DM, diabetes mellitus; PBS, phosphate-buffered saline.

the pathophysiological state of type II DM in humans, consistent with previous results [12,18].

Assessment of voiding function

Representative cystometric graphs of rats displaying normal and abnormal voiding patterns are shown in Fig. 2A and B. All rats in the N+PBS group ($n=10$) manifested a normal voiding pattern, with a voiding frequency of 8 to 9 times per 30 min during cystometry. During each voiding episode, the net baseline bladder pressure gradually increased from 0 to ~10 cmH_2O before peaking at 38.9±9.3 cmH_2O, and a discrete amount of 0.4±0.14 mL voided saline was recorded with each bladder contraction. Some rats in the DM+PBS group ($n=6$) manifested an abnormal pattern, with a voiding frequency of 1 to 2 times per 30 min. The net baseline bladder pressure gradually increased from 0 to ~20 cmH_2O before peaking at 50.0±10.8 cmH_2O, with a discrete voided amount of 3.74±1.09 mL. Besides, in the current study, a small number of rats manifested another 2 abnormal cystometric patterns (Fig. 2C, D): acontractile bladder (only 1 rat in DM+PBS group) and detrusor overactivity (2 rats, 2 rats, 1 rat in DM+PBS, DM+T, and DM+B group, respectively). Acontractile bladder pattern was defined as continuous or intermittent urine leakage without obvious detrusor contractions during the filling phase, whereas detrusor overactivity pattern was defined as shorter

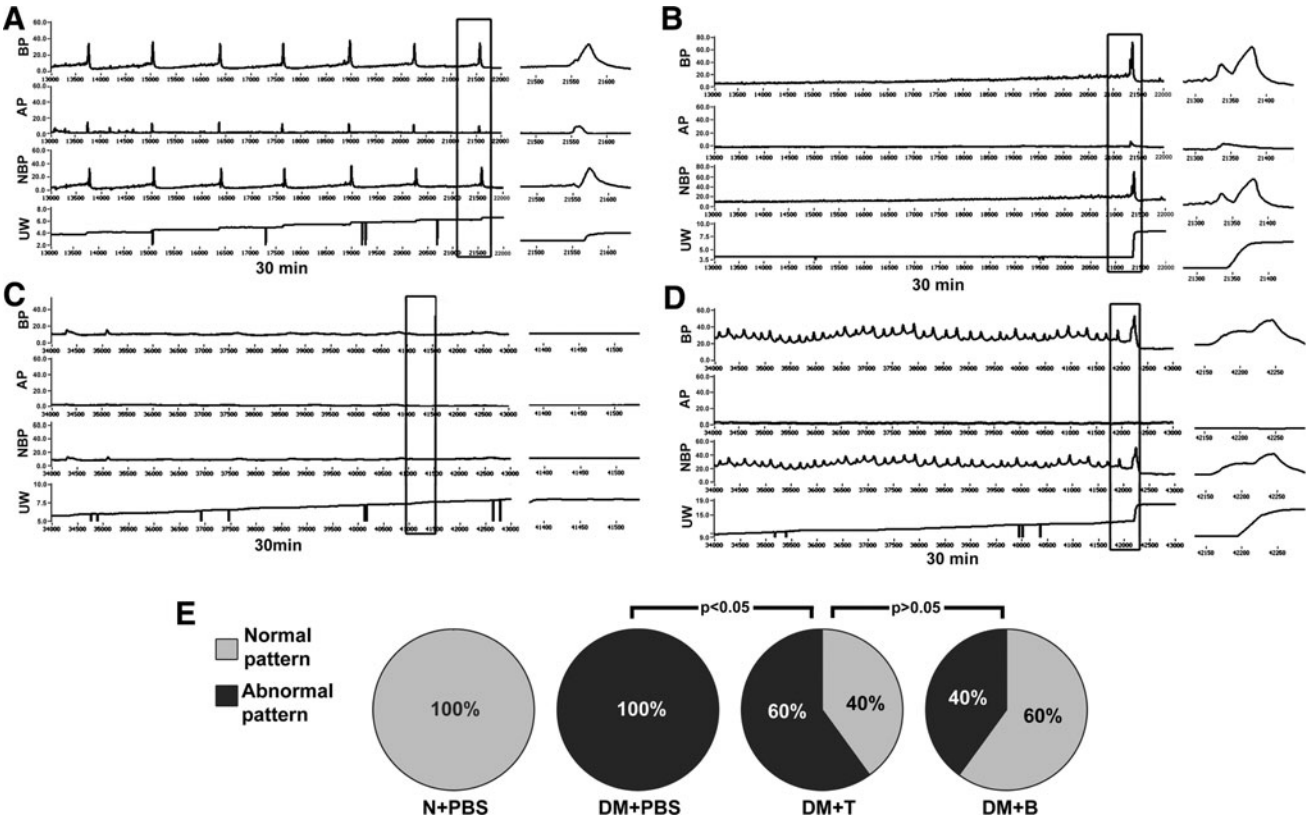

FIG. 2. Assessment of voiding function with conscious cystometry. **(A)** Normal voiding pattern was noted in 10 rats of N+PBS group, 4 rats of DM+T group, and 6 rats of DM+B group. **(B)** Abnormal voiding pattern was noted in 6 rats of DM+PBS group, 4 rats of DM+T group, and 3 rats of DM+B group. **(C)** A contractile bladder pattern (1 rat of DM+PBS group) and **(D)** detrusor overactivity pattern (2 rats of DM+PBS group, 2 rats of DM+T group, 1 rat of DM+B group) were also regarded as abnormal cystometry. Boxed areas of left panels are enlarged into right panels, respectively. **(E)** Normal voiding pattern was significantly more common ($P<0.05$) in the DM+T and DM+B groups compared with the DM+PBS group. BP: bladder pressure (cmH_2O). AP: abdomen pressure (cmH_2O). NBP: net bladder pressure (cmH_2O). UW: urine weight (g). DM, diabetes mellitus; PBS, phosphate-buffered saline.

Table 2. Comparison of Voiding Behaviors in Conscious Cystometry

Groups	*N+PBS*	*DM+PBS*	*DM+T*	*DM+B*	P *value*
Micturition interval (s)	327.4±98.7[a]	1799.3±219.4[b]	1294.0±371.2	1147.9±539.6	<0.001
Urine volume per void (mL)	0.4±0.14[a]	3.74±1.09[a]	2.23±0.32	1.85±0.72	<0.001
Maximum voiding pressure (cmH_2O)	38.9±9.3[c]	50.0±10.8	46.1±11.2	45.3±11.4	=0.116
Residual volume (mL)	0.01±0.02[a]	0.20±0.04	0.21±0.02	0.19±0.03	<0.001

[a] $P<0.001$ versus other groups.
[b] $P<0.05$ versus DM+T and DM+B.
[c] $P<0.05$ versus DM+PBS.

micturition intervals and smaller micturition volume per void compared with normal pattern. A significant proportion of the diabetic rats that received ADSCs transplantation had normal voiding patterns (40% of the DM+T group and 60% of the DM+B group compared with 0% of the DM+PBS group, $P<0.05$, Fig. 2E). The significantly ($P<0.05$) shorter micturition intervals and smaller urine volume in both DM+T and DM+B relative to DM+PBS (Table 2) suggest that contractile function of bladder is preserved after ADSCs injection regardless of the route of administration.

Tracking of EdU-positive cells

Histological examination after 1 month revealed EdU labeled cells in the bladder submucosal and muscular layers (Fig. 3A). A few EdU positive nuclei appeared to be

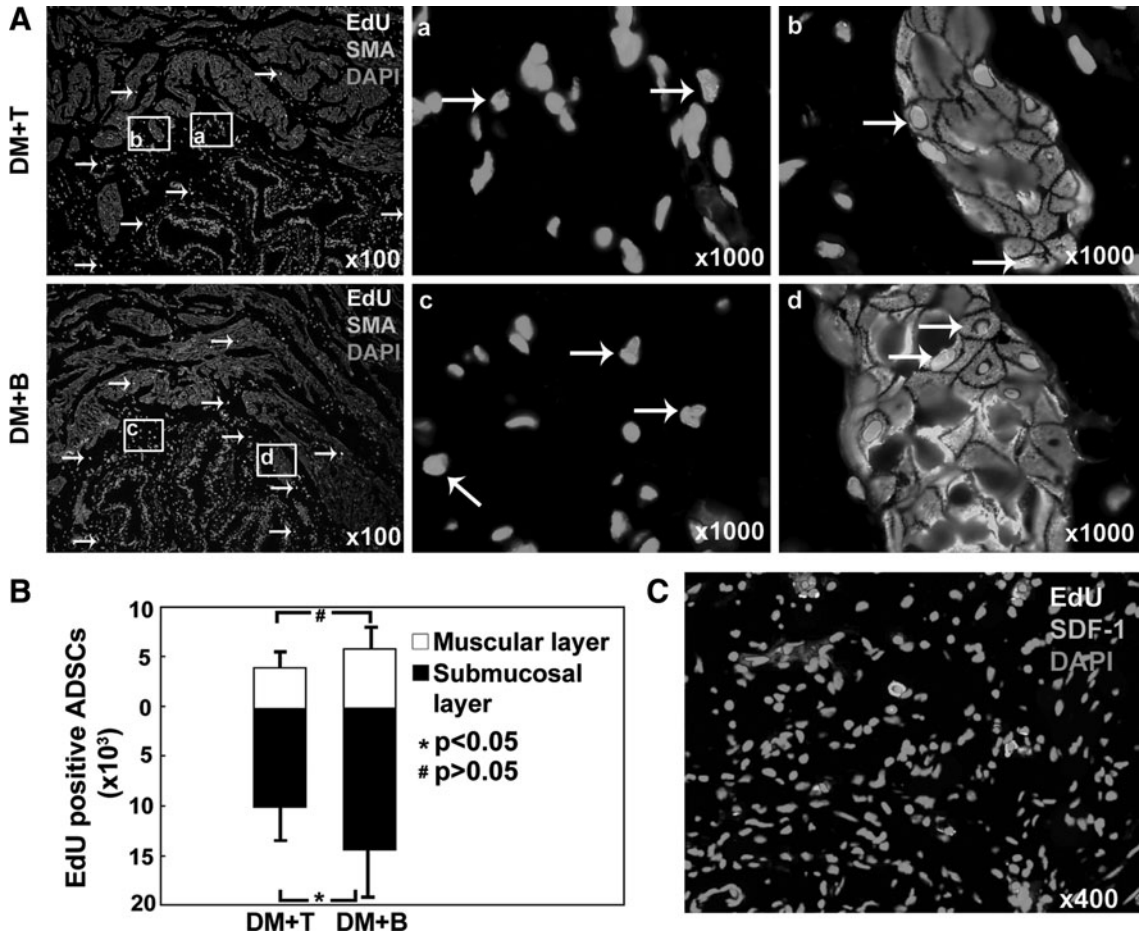

FIG. 3. Tracking of EdU-labeled ADSCs and identification of SDF-1 expression in the bladder. **(A)** EdU-positive ADSCs were located mainly in muscular and submucosal layers (*white arrow*). Please note that some EdU colocalized with SMA. Boxed areas in the ×100 graphs are shown in the corresponding ×1,000 graphs. **(B)** The number of EdU-positive ADSCs in the whole bladder was counted and calculated by computer software. They only accounted for a small fraction of original transplanted ADSCs. **(C)** Bladder tissue from DM+T group was stained with SDF-1 antibody. Expression of SDF-1 was clearly detected in the bladder tissue sections. ADSC, adipose tissue-derived stem cell; EdU, 5-ethynyl-2-deoxyuridine; SMA, smooth muscle actin; SDF-1, stromal cell-derived factor-1.

colocalized with SMA staining. In the DM + T group, $\sim 4.7 \pm 2.1 \times 10^3$ and $10.2 \pm 3.8 \times 10^3$ EdU-positive cells were localized to muscular layer and submucosal layer, respectively. In the DM + B group, $5.6 \pm 2.9 \times 10^3$ and $14.9 \pm 5.0 \times 10^3$ EdU-positive cells were localized to the muscular layer and submucosal layer, respectively (Fig. 3B). Expression of SDF-1 was clearly identified in the bladder tissue of DM + T group (Fig. 3C).

Quantification of apoptosis

Only cells positive for both TUNEL and DAPI were considered positive for apoptosis. Apoptotic cells were predominantly located in the mucosal layer and muscular layer (Fig. 4A). Apoptosis was significantly more abundant in DM + PBS animals compared with nondiabetic animals (Fig. 4B). Animals treated with ADSCs had a significantly less apoptotic cells in mucosal layer relative to DM + PBS animals ($P < 0.05$); no significant difference in the muscular layer was detected.

For cultured rat urothelial cells, significantly more ($P < 0.001$) apoptosis was observed in cells treated with high glucose (HG group, 30.3% ± 9.9%) versus those treated with normal glucose (NG group, 5.1% ± 0.8%). Significantly less ($P < 0.001$) apoptosis was found in the cells treated with high glucose in rat ADSCs conditioned medium (HG + ADSCs CM group, 10.1% ± 2.7%) versus HG group. No significant difference in the cells treated with high glucose in rat PSMCs conditioned medium (HG + PSMCs CM group, 33.4% ± 8.1%) was detected compared with HG group. For cultured rat bladder SMCs, flow cytometry analysis showed significantly more ($P < 0.001$) apoptosis in HG group (19.1% ± 4.9%) versus NG group (1.6% ± 0.7%), significantly lower ($P < 0.05$) in HG + ADSCs CM group (10.3% ± 4.6%) versus HG group, and no significant difference in HG + PSMCs group (20.0% ± 9.8%) versus HG group (Fig. 4C, Supplementary

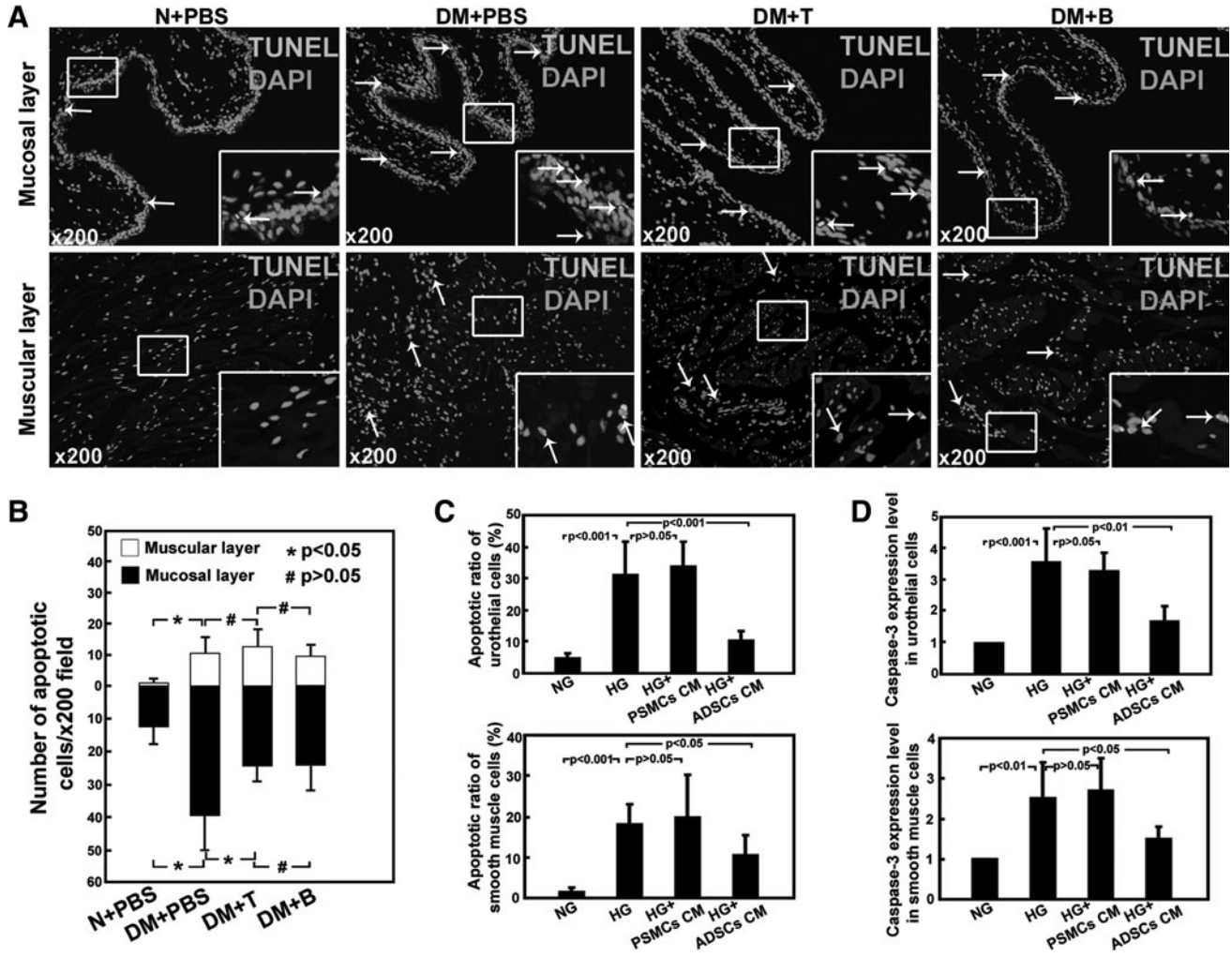

FIG. 4. Quantification of apoptosis. **(A)** Only cells positive for both TUNEL and DAPI were considered positive for apoptosis (*white arrow*). Apoptotic cells were located predominantly in mucosal layer compared with muscular layer in all groups. **(B)** Quantification of the apoptotic nuclei per × 200 magnification field was analyzed by Image Pro Plus software. Significantly less apoptosis was noted in groups that received an injection of ADSCs. **(C)** The percentage of apoptosis in cultured cells with different treatments was evaluated. **(D)** Gene Caspase-3 expression in cultured cells was analyzed with real-time PCR. NG: regular medium with normal glucose. HG: regular medium with high glucose. HG + PSMCs CM: rat penile smooth muscle cells conditioned medium with high glucose. HG + ADSCs CM: rat ADSCs conditioned medium with high glucose. DAPI, 4′,6-diamidino-2-phenylindole.

Figs. S1A and S2A). TUNEL positive cells could be observed in the cultured urothelial cells and SMCs (Supplementary Figs. 1B and 2B).

For cultured rat urothelial cells, real-time PCR analysis demonstrated significantly higher level Caspase-3 expression in HG group versus NG group ($P < 0.001$), significantly lower level in HG + ADSCs CM group versus HG group ($P < 0.01$), and no significant difference in HG + PSMCs CM group versus HG group ($P > 0.05$). For cultured rat SMCs, real-time PCR analysis demonstrated significantly higher level Caspase-3 expression in HG group versus NG group ($P < 0.01$), significantly lower level in HG + ADSCs CM group versus HG group ($P < 0.05$), and no significant difference in HG + PSMCs CM group versus HG group ($P > 0.05$) (Fig. 4D).

Quantification of vascularity

In normal rats, a dense and continuous network of Col IV-positive capillaries was detected below the urothelium (Fig. 5A), and UP II, a specific differentiation product of urothelial cells, was distributed as a dense layer on the luminal surface of the umbrella cells (Supplementary Fig. S3). In DM + PBS, both Col IV-positive capillaries network and UP II layer lost continuity, deficient in some area or became very thin in other areas. After treatment with ADSCs, both the damaged Col IV staining and UP II staining were improved. RECA-1 staining was intensely positive in the submucosal layer of N + PBS, DM + T, and DM + B with minimal positivity in DM + PBS (Fig. 5B, C).

VEGF quantification assay in the current study (Fig. 5D) revealed that ADSCs secreted significantly higher VEGF than PSMCs (652.1 ± 140.3 pg/mL in ADSCs conditioned medium, 348.8 ± 96.7 pg/mL in PSMCs conditioned medium, $P < 0.05$), thus suggesting that ADSCs exerted their angiogenesis effect at least partly through VEGF.

Matrigel-based capillary-like tube formation assay in vitro showed significantly upregulated human umbilical vein endothelial cells' (HUVECs) ability to form endothelial-like tubes in HG + ADSCs CM group versus HG group ($P < 0.01$), whereas no significant effects were observed in HG + PSMCs CM group ($P > 0.05$) (Fig. 6).

Discussion

A number of animal models for type II diabetes in humans have been developed; however, models that utilized just one means of inducing the diabetic state may not be reflective of the human condition [12]. Diabetes in humans may be related to genetic, environmental, dietary, autoimmune, and possibly other occult causes. Therefore, we adapted the approach developed by Zhang et al. and Srinivasan et al. [12,18], in which rats were fed with HFD and then given multiple low-dose STZ to simulate the initiation and progressing of type II DM in humans.

Voiding dysfunction in humans with diabetes may take the form of sensory deficit and poor contractility from a hypocontractile bladder or an overactive bladder syndrome typically described as urgency and frequency, with or without incontinence [19]. In the current study, rats in the DM + PBS group had cystometric findings most consistent with hypocontractile bladders. According to Daneshgari's proposal of "temporal theory of DBD" [1], our rat model is, hence, consistent with end-stage DBD.

Based on cystometric analysis, we found that all the rats in the DM + PBS group had voiding dysfunction, whereas only 60% and 40% in the DM + T and DM + B groups, respectively, had voiding dysfunction 1 month after ADSCs injection. In humans, DBD is a progressive disease, and there is no cure at present. The fact that tail vein injection of ADSCs ameliorates bladder dysfunction in 40% of rats was beyond our expectations, because we did not expect that an intravenous injection would work for the bladder. We are also happy to see 60% of rats in the direct bladder injection group normally void, because these rats continue to be hyperglycemic and hyperlipidemic after ADSCs treatment. In our previous study, we have noted a progressive deterioration of both function and histology of the bladder in these rats. It is likely that repeated ADSCs treatments and correction of hyperglycemia and hyperlipidemia may be needed to achieve better results. This will be the subject of another study.

It remains unclear how the transplanted ADSCs improve bladder function. In the DM + T group, injected ADSCs were able to be localized to the bladder. This may be attributable to homing factors such as SDF-1, as ADSCs have been shown to express the SDF-1 receptor CXCR4 and migrate to SDF-1 in cell migration assays [20]. In our previous in vivo study, SDF-1/CXCR4 also appears to mediate migration of ADSCs toward prostate tumor in mice [21]. However, without blockade examinations, it cannot be conclusively demonstrated that SDF-1 mediates this effect in the current study. After the tail vein injection, it is expected that ADSCs migrate to many organs in the body. In a rat model of cavernous nerve injury, we detected ADSCs in lungs, liver, prostate, spleen, major pelvic ganglia, penis, and bone marrow after an injection into the corpus cavernosum. After 28 days, most of the ADSCs were cleared from other organs and moved to the bone marrow to be reserved cells.

In the current study, we used EdU labeling as a tracking method, which is incorporated into the nuclear DNA and, therefore, makes it easier to colocalize with DAPI [22]. EdU was incorporated into the nucleus in ~50% of ADSCs with this labeling system [22]. In both the DM + T and DM + B groups, EdU-labeled cells in the bladder demonstrated the capacity of ADSCs to survive for at least 1 month post-transplantation. EdU-expressing ADSCs were observed to be predominantly localized in the submucosa, and some of the EdU-positive nuclei appeared to reside within cells expressing SMA, thus suggesting that a small fraction of the transplanted ADSCs may have differentiated into SMCs. Time-dependent decline in ADSCs number after injection into the corpus cavernosum has been previously reported and suggests that the beneficial effects of ADSCs are established early after injection [9]. The relative paucity of EdU positive cells in the bladders of these animals after 1 month suggests that the differentiation pathway plays at most a minor role in the therapeutic effect of ADSCs. One explanation is the immortal strand hypothesis [23]. Labeled DNA in dividing cells will be quickly diluted by cell divisions but will be retained for much longer periods in slowly dividing stem cells. If the segregation of sister chromatids into stem cell daughters is not random, and if the stem cell retains the older unlabeled template strands, then the stem cell will lose all labels by the second division after administration of the label as a pulse.

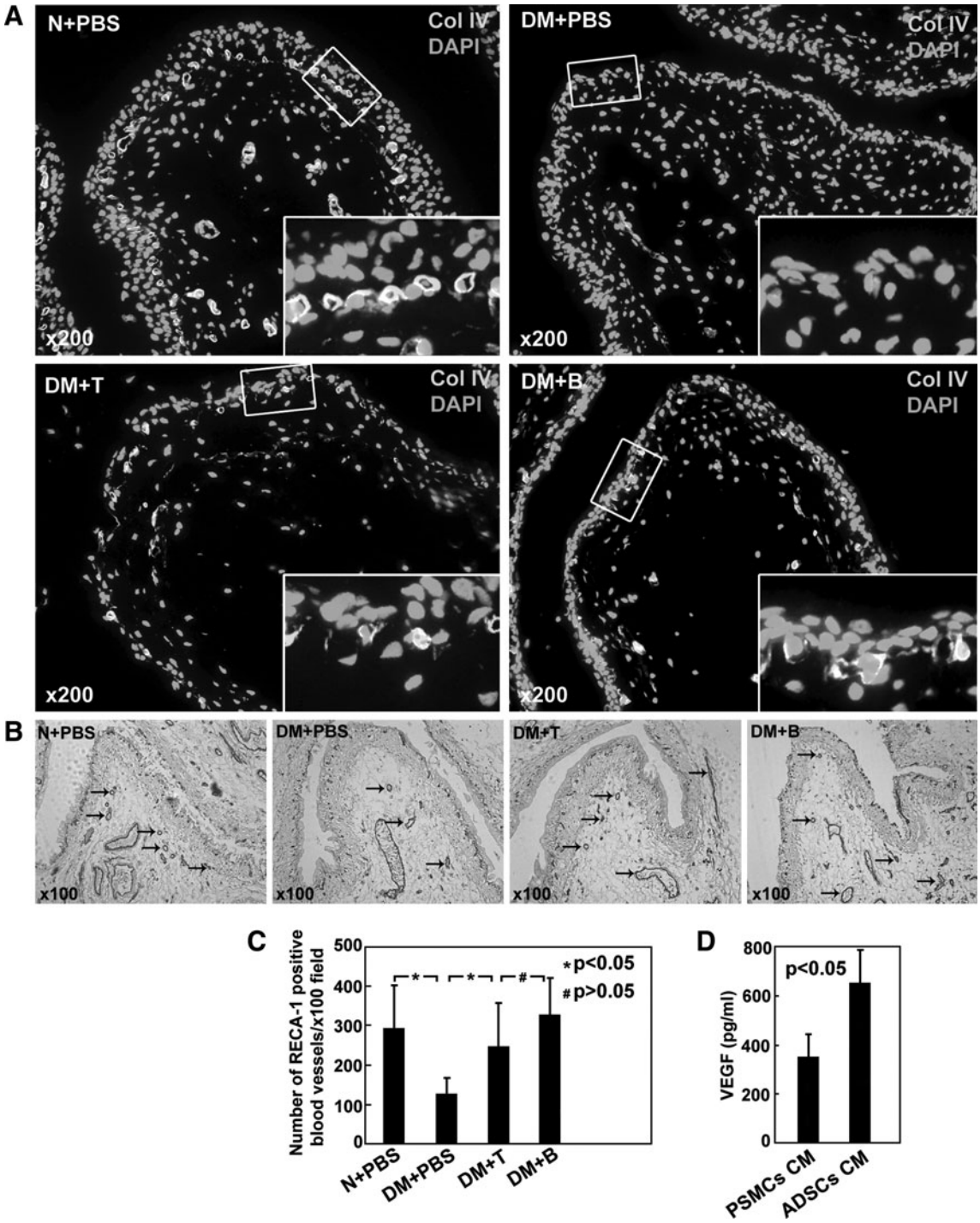

FIG. 5. **(A)** Collagen IV staining demonstrated a "suburothelial capillary network" located directly below the urothelium. This network was densely stained and continuous in N + PBS, and was fragmented in DM + PBS. The network integrity was greater in DM + T and DM + B groups relative to the DM + PBS group. **(B)** RECA-1 staining (*black arrow*) revealed that DM + T and DM + B group had a greater density of blood vessels compared with the DM + PBS group. **(C)** The number of RECA-1 positive blood vessels was assessed. The blood vessel content was greater in DM + T and DM + B groups relative to the DM + PBS group ($P < 0.05$). **(D)** Vascular endothelial growth factor secretion in the conditioned media of ADSCs and PSMCs was quantified by enzyme-linked immunosorbent assay. Each bar represents the average of 3 independent experiments, and each measurement was done in triplicate. PSMCs CM: rat penile smooth muscle cells conditioned medium. ADSCs CM: rat ADSCs conditioned medium. RECA-1, rat endothelial cell antigen-1.

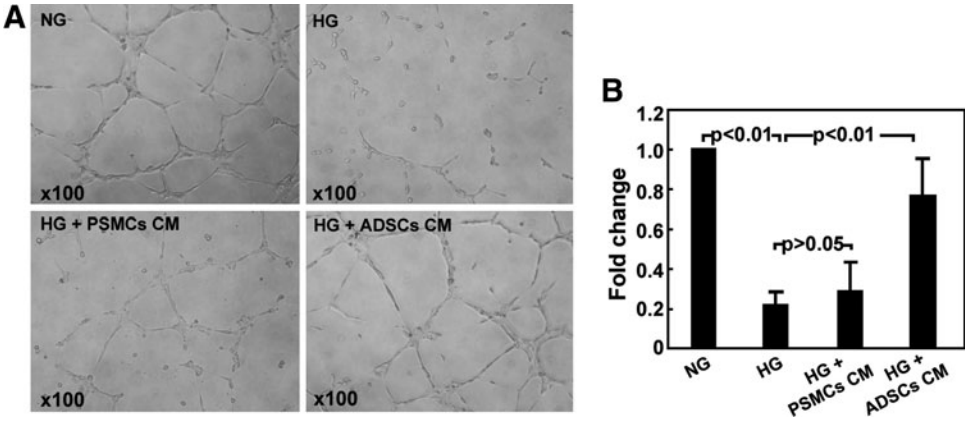

FIG. 6. Matrigel-based capillary-like tube formation assay. **(A)** Representative photographs of tube-like structures. **(B)** Differences in the number of endotubes among different treatments are presented as fold change. NG: regular medium with normal glucose. HG: regular medium with high glucose. HG + PSMCs CM: human penile smooth muscle cells conditioned medium with high glucose. HG + ADSCs CM: human ADSCs conditioned medium with high glucose.

Since cellular differentiation appears to play a minor role in the therapeutic effects of ADSCs in this system, it is logical to hypothesize that paracrine release of cytokines and growth factors by transplanted ADSCs or their neighboring cells is responsible for the observed effects. It has been shown that secretion of bioactive materials by MSCs in response to injury mitigates the inflammatory response and, in turn, decreases injury and promotes repair [24,25]. Inhibition of apoptosis is one of the downstream results of such bioactive agents. ADSCs have demonstrated efficacy in reduction of apoptosis in corporal tissue after cavernous nerve injury, and a similar effect might be at work in this system [8]. The underlying mechanisms may involve the secretion of VEGF, insulin-like growth factor I), and hepatocyte growth factor by ADSCs [26,27].

Angiogenic and vascular restorative properties of ADSCs by intravenous or local administration have been noted in previous in vivo studies [26,28]. Preservation of vascular integrity has been associated with improved voiding function in a hyperlipidemic rat model of detrusor overactivity [10]. In an in vitro culture system, ADSCs conditioned medium could enhance angiogenesis in hypoxic conditioning [29]. In the current study, ADSCs conditioned medium could also promote capillary-like tube formation in high-glucose conditioning. ADSCs are known to secrete VEGF and CXCL5 at higher rates than other cell types [30]. The ADSC-enhanced angiogenesis in a cultured rat aortic ring model was blocked by a VEGF blocker [31]. CXCL5 serves as chemoattractant to ADSCs and HUVECs, and upregulates HUVECs ability to form capillary-like tubes [17]. In the current study, we found some evidence that "suburothelial capillaries network" might be essential for the normal physiological properties of urothelium. Further, VEGF and CXCL5 secreting properties of ADSCs may under-estimate the suburothelial protective effects of ADSCs therapy.

It is interesting that differences in the rate of abnormal bladder function differed a little between the DM + B and DM + T groups. The lack of significant difference may be due, in part, to the small sample size. The optimal means for administration of ADSCs remains open to further research. Further, it is unclear whether ADSCs harvested before development of the diabetic state may exert a more powerful effect. The concept of "metabolic memory" [32] suggests that ADSCs derived from diabetic animals might behave differently than those derived from healthy animals. Be that as it may, it seems most likely that only individuals with a metabolic derangement leading to tissue damage will seek out this form of treatment. Hence, the diabetic or other systemically ill animal models are appropriate research subjects for preclinical research.

In conclusion, ADSCs transplantation ameliorates voiding dysfunction in a rat model of type II diabetes created by a HFD and low-dose STZ. ADSCs may exert effects partly due to differentiation into SMCs, but paracrine effects seem more likely an explanation for observed improvements. Inhibition of apoptosis and promotion of vascular integrity may be the most important functional changes after ADSCs treatment.

Acknowledgments

This work was supported by grants from the National Institutes of Health (NIDDK, P50-DK64538, R37 DK045370, and R01 DK069655).

Author Disclosure Statement

The authors have nothing to disclose, and no competing financial interests exist.

References

1. Daneshgari F, G Liu, L Birder, AT Hanna-Mitchell and S Chacko. (2009). Diabetic bladder dysfunction: current translational knowledge. J Urol 182:S18–S26.
2. Yoshimura N, MB Chancellor, KE Andersson and GJ Christ. (2005). Recent advances in understanding the biology of diabetes-associated bladder complications and novel therapy. BJU Int 95:733–738.
3. Zhao W, C Zhang, C Jin, Z Zhang, D Kong, W Xu and Y Xiu. (2010). Periurethral injection of autologous adipose-derived stem cells with controlled-release nerve growth factor for the treatment of stress urinary incontinence in a rat model. Eur Urol 59:155–163.
4. Sasaki K, MB Chancellor, WF Goins, MW Phelan, JC Glorioso, WC de Groat and N Yoshimura. (2004). Gene therapy using replication-defective herpes simplex virus vectors expressing nerve growth factor in a rat model of diabetic cystopathy. Diabetes 53:2723–2730.
5. Saito M, Y Kinoshita, I Satoh, C Shinbori, H Suzuki, M Yamada, T Watanabe and K Satoh. (2007). Ability of cyclohexenonic

long-chain fatty alcohol to reverse diabetes-induced cystopathy in the rat. Eur Urol 51:479–487; discussion 487–478.
6. Zuk PA, M Zhu, H Mizuno, J Huang, JW Futrell, AJ Katz, P Benhaim, HP Lorenz and MH Hedrick. (2001). Multilineage cells from human adipose tissue: implications for cell-based therapies. Tissue Eng 7:211–228.
7. Lin G, M Garcia, H Ning, L Banie, YL Guo, TF Lue and CS Lin. (2008). Defining stem and progenitor cells within adipose tissue. Stem Cells Dev 17:1053–1063.
8. Albersen M, TM Fandel, G Lin, G Wang, L Banie, CS Lin and TF Lue. (2010). Injections of adipose tissue-derived stem cells and stem cell lysate improve recovery of erectile function in a rat model of cavernous nerve injury. J Sex Med 7:3331–3340.
9. Huang YC, H Ning, AW Shindel, TM Fandel, G Lin, AM Harraz, TF Lue and CS Lin. (2010). The effect of intracavernous injection of adipose tissue-derived stem cells on hyperlipidemia-associated erectile dysfunction in a rat model. J Sex Med 7:1391–1400.
10. Huang YC, AW Shindel, H Ning, G Lin, AM Harraz, G Wang, M Garcia, TF Lue and CS Lin. (2010). Adipose derived stem cells ameliorate hyperlipidemia associated detrusor overactivity in a rat model. J Urol 183:1232–1240.
11. Garcia MM, TM Fandel, G Lin, AW Shindel, L Banie, CS Lin and TF Lue. (2010). Treatment of erectile dysfunction in the obese type 2 diabetic ZDF rat with adipose tissue-derived stem cells. J Sex Med 7:89–98.
12. Zhang M, XY Lv, J Li, ZG Xu and L Chen. (2008). The characterization of high-fat diet and multiple low-dose streptozotocin induced type 2 diabetes rat model. Exp Diabet Res 2008:704045.
13. Bunnell BA, M Flaat, C Gagliardi, B Patel and C Ripoll. (2008). Adipose-derived stem cells: isolation, expansion and differentiation. Methods (San Diego, Calif 45:115–120.
14. Dubois SG, EZ Floyd, S Zvonic, G Kilroy, X Wu, S Carling, YD Halvorsen, E Ravussin and JM Gimble. (2008). Isolation of human adipose-derived stem cells from biopsies and liposuction specimens. Methods Mol Biol (Clifton, NJ) 449:69–79.
15. Malmgren A, C Sjogren, B Uvelius, A Mattiasson, KE Andersson and PO Andersson. (1987). Cystometrical evaluation of bladder instability in rats with infravesical outflow obstruction. J Urol 137:1291–1294.
16. Albersen M, TM Fandel, H Zhang, L Banie, G Lin, D De Ridder, CS Lin and TF Lue. (2011). Pentoxifylline promotes recovery of erectile function in a rat model of postprostatectomy erectile dysfunction. Eur Urol 59:286–296.
17. Zhang H, H Ning, L Banie, G Wang, G Lin, TF Lue and CS Lin. (2010). Adipose tissue-derived stem cells secrete CXCL5 cytokine with chemoattractant and angiogenic properties. Biochem Biophys Res Commun 402:560–564.
18. Srinivasan K, B Viswanad, L Asrat, CL Kaul and P Ramarao. (2005). Combination of high-fat diet-fed and low-dose streptozotocin-treated rat: a model for type 2 diabetes and pharmacological screening. Pharmacol Res 52:313–320.
19. Goldstraw MA, MG Kirby, J Bhardwa and RS Kirby. (2007). Diabetes and the urologist: a growing problem. BJU Int 99:513–517.
20. Kim JH, MR Lee, JH Kim, MK Jee and SK Kang. (2008). IFATS collection: selenium induces improvement of stem cell behaviors in human adipose-tissue stromal cells via SAPK/JNK and stemness acting signals. Stem Cells (Dayton, Ohio) 26:2724–2734.
21. Lin G, R Yang, L Banie, G Wang, H Ning, LC Li, TF Lue and CS Lin. (2010). Effects of transplantation of adipose tissue-derived stem cells on prostate tumor. Prostate 70:1066–1073.
22. Lin G, YC Huang, AW Shindel, L Banie, G Wang, TF Lue and CS Lin. (2009). Labeling and tracking of mesenchymal stromal cells with EdU. Cytotherapy 11:864–873.
23. Rando TA. (2007). The immortal strand hypothesis: segregation and reconstruction. Cell 129:1239–1243.
24. Caplan AI. (2007). Adult mesenchymal stem cells for tissue engineering versus regenerative medicine. J Cell Physiol 213:341–347.
25. Prockop DJ. (2009). Repair of tissues by adult stem/progenitor cells (MSCs): controversies, myths, and changing paradigms. Mol Ther 17:939–946.
26. Rehman J, D Traktuev, J Li, S Merfeld-Clauss, CJ Temm-Grove, JE Bovenkerk, CL Pell, BH Johnstone, RV Considine and KL March. (2004). Secretion of angiogenic and antiapoptotic factors by human adipose stromal cells. Circulation 109:1292–1298.
27. Sadat S, S Gehmert, YH Song, Y Yen, X Bai, S Gaiser, H Klein and E Alt. (2007). The cardioprotective effect of mesenchymal stem cells is mediated by IGF-I and VEGF. Biochem Biophys Res Commun 363:674–679.
28. Moon MH, SY Kim, YJ Kim, SJ Kim, JB Lee, YC Bae, SM Sung and JS Jung. (2006). Human adipose tissue-derived mesenchymal stem cells improve postnatal neovascularization in a mouse model of hindlimb ischemia. Cell Physiol Biochem 17:279–290.
29. Efimenko A, E Starostina, N Kalinina and A Stolzing. (2011). Angiogenic properties of aged adipose derived mesenchymal stem cells after hypoxic conditioning. J Transl Med 9:10.
30. Zhang H, R Yang, Z Wang, G Lin, TF Lue and CS Lin. (2011). Adipose tissue-derived stem cells secrete CXCL5 cytokine with neurotrophic effects on cavernous nerve regeneration. J Sex Med 8:437–446.
31. Rasmussen JG, O Frobert, L Pilgaard, J Kastrup, U Simonsen, V Zachar and T Fink. (2011). Prolonged hypoxic culture and trypsinization increase the pro-angiogenic potential of human adipose tissue-derived stem cells. Cytotherapy 13:318–328.
32. Ceriello A, MA Ihnat and JE Thorpe. (2009). Clinical review 2: the "metabolic memory": is more than just tight glucose control necessary to prevent diabetic complications? J Clin Endocrinol Metab 94:410–415.

Address correspondence to:
Dr. Tom F. Lue
Knuppe Molecular Urology Laboratory
Department of Urology
School of Medicine
University of California, San Francisco
400 Parnassus Avenue, Suite A-633
San Francisco, CA 94143-0738

E-mail: tlue@urology.ucsf.edu

Received for publication May 12, 2011
Accepted after revision August 27, 2011
Prepublished on Liebert Instant Online October 18, 2011